29. Grigera, S. A. *et al.* Magnetic field-tuned quantum criticality in the metallic ruthenate $Sr_3Ru_2O_7$. *Science* **294**, 329–332 (2001).

**Acknowledgements** The work at the National High Magnetic Field Laboratory was supported by the National Science Foundation and the DOE Office of Science. We thank S. Chakravarty, S. A. Kivelson, P.A. Lee, R. Ramazashvili, C. M. Varma, I. Vekhter and F.-C. Zhang for discussions.

**Competing interests statement** The authors declare that they have no competing financial interests.

**Correspondence** and requests for materials should be addressed to F.F.B. (fedor@lanl.gov).

# Epoxidation of polybutadiene by a topologically linked catalyst

**Pall Thordarson, Edward J. A. Bijsterveld, Alan E. Rowan & Roeland J. M. Nolte**

*Department of Organic Chemistry, NSRIM, University of Nijmegen, Toernooiveld 1, 6525 ED, Nijmegen, The Netherlands*

**Nature has evolved complex enzyme architectures that facilitate the synthesis and manipulation of the biopolymers DNA and RNA, including enzymes capable of attaching to the biopolymer substrate and performing several rounds of catalysis before dissociating[1–5]. Many of these 'processive' enzymes have a toroidal shape and completely enclose the biopolymer while moving along its chain, as exemplified by the DNA enzymes T4 DNA polymerase holoenzyme[6] and λ-exonucleoase[7]. The overall architecture of these systems resembles that of rotaxanes, in which a long molecule or polymer is threaded through a macrocycle. Here we describe a rotaxane that mimics the ability of processive enzymes to catalyse multiple rounds of reaction while the polymer substrate stays bound. The catalyst consists of a substrate binding cavity incorporating a manganese(III) porphyrin complex that oxidizes alkenes within the toroid cavity, provided a ligand has been attached to the outer face of the toroid to both activate the porphyrin complex and shield it from being able to oxidize alkenes outside the cavity. We find that when threaded onto a polybutadiene polymer strand, this catalyst epoxidizes the double bonds of the polymer, thereby acting as a simple analogue of the enzyme systems.**

Rotaxanes and the topologically related catenanes are of interest since these mechanically interlocked assemblies represent a unique form of bonding. They have been shown to function as "molecular motors"[8–11], "molecular shuttles"[12], "molecular muscles"[13], and even as active components in electronic devices[14]. Polyrotaxanes can be prepared by statistically threading toroids, namely cyclodextrins and crown ethers, onto polymers such as polyethyleneglycol[15] and polyurethane[16]. Until now, no examples of catalytically active rotaxanes have been reported. With the natural processive enzymes in mind, we have designed a rotaxane catalytic system in which a cavity containing porphyrin (**Mn1**) is threaded onto a polybutadiene polymer (**PD**) and can move along it while catalysing the conversion of the double bonds in the thread into the corresponding epoxide functions (Fig. 1a).

The toroidal catalyst used is based on a glycoluril clip molecule[17,18] that is capped with a manganese(III) porphyrin complex (**Mn1**, Figs 1 and 2), resulting in a macrocyclic compound with a central cavity in which substrates can bind. Manganese(III) porphyrins have been investigated extensively as oxidative catalysts, most prominently in the epoxidation of alkenes[19]. In the presence of an oxygen donor, for example, iodosylbenzene (PhIO) or sodium hypochlorite (NaOCl) and an activating axial ligand, a Mn(V) = O species is formed, which transfers its oxygen to the substrate (alkene) to form the product[19].

The porphyrin **Mn1** has previously been shown to be an excellent catalyst for the conversion of alkenes to epoxides[20]. In the presence of a small ligand such as pyridine (**py**), which binds in the cavity, catalysis occurs on the 'outside' of this catalyst (approach A in Fig. 1b). When a bulky axial ligand such as *tert*-butylpyridine (**tbpy**), which can only bind to the 'outside' of **Mn1**, is used, the catalysis occurs predominantly inside the cavity (approach B in Fig. 1b). To investigate whether **Mn1** could mimic the action of

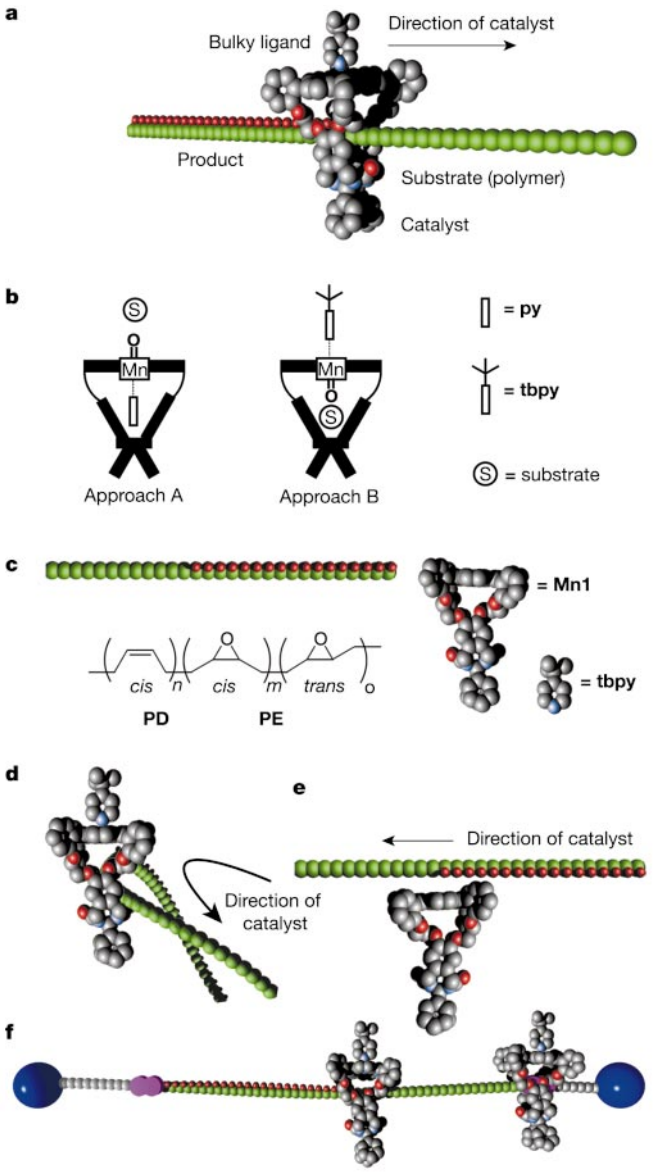


**Figure 1** The various catalytic architectures discussed in this work. **a**, Schematic representation of the toroidal catalyst **Mn1** encircling a polybutadiene substrate and converting it into the product. **b**, Two ways in which catalyst **Mn1** can act as an epoxidation catalyst in combination with ligands **py** and **tbpy**. **c**, Structural representation of polybutadiene **PD**, the product **PE**, the **Mn1** catalyst, and the ligand **tbpy**. **d**, Schematic representation of the 'loop' mechanism where the substrate folds into the cavity of **Mn1**. **e**, Schematic representation of the 'outside' mechanism where the substrate reacts on the 'outside' (top) of **Mn1**. **f**, Schematic representation of the catalytically active rotaxane **Mn3**.

processive enzymes and carry out catalysis on a polymer in a rotaxane-like architecture, that is, in which the polymer substrate is threaded through the macrocycle, this complex was tested as a catalyst for the conversion of polybutadiene (**PD**) into polybutadieneepoxide (**PE**)[21]. In the presence of **tbpy** as ligand, which forces catalysis to occur in the cavity, and PhIO as an oxidant, the relative rates of conversion of **PD** into **PE** were compared to **Mn2** (Table 1, entries 1–5). This latter catalyst is electronically related to **Mn1** but does not possess a binding cavity. $^1$H NMR analysis of the products (only epoxides were formed[22]) revealed that **Mn1** is a slower catalyst (by a factor of 2.2, compare entries 1 and 3) than **Mn2** for the conversion of **PD** to **PE**. This reduced activity is not unexpected since the reaction of **PD** is forced to take place inside the cavity of **Mn1** (Fig. 1a, b). When the cavity of **Mn1** was intentionally blocked by the addition of 1 equiv. of viologen **V** ($K_{ass} > 10^5\,M^{-1}$)[18], which acts as an inhibitor (Supplementary Information), the reaction rate dropped significantly (by ~40%, compare entries 1 and 2). This is in contrast to control experiments with **Mn2**, where it was shown that **V** actually activates this simple catalyst (compare entries 3 and 4)[23].

When the concentration of all the reagents was lowered, the rate of epoxidation using **Mn1** dropped accordingly (compare entries 1 and 5 in Table 1), see below. Moreover, while toroidal catalyst **Mn1** produced 80% *trans*- and 20% *cis*-epoxide polymer from **PD** (>98% *cis*-butadiene), **Mn2** gave predominantly the *cis*-product (78% *cis*, 22% *trans*, see Table 2). This large difference in stereoselectivity strongly suggests that in the case of **Mn1**, catalysis occurs in the sterically demanding cavity, as shown previously in our work with simpler substrates such as stilbenes[20].

Taken together, these observations suggest that **Mn1** forms a pseudo-rotaxane complex with the **PD** polymer and then acts as a topologically linked catalyst (Fig. 1a). Two other possible mechanisms could also (partly) explain the experimental results. One involves folding of the polymer substrate and bending inside the cavity of **Mn1** (Fig. 1d), the other, reaction of **PD** on the 'outside' of **Mn1** (Fig. 1e). Simple molecular modelling suggests that the first of these two possibilities is unlikely owing to the large steric bulk of the polymer, while the second possibility should only play a minor role in the presence of an excess of **tbpy** (Supplementary Information).

To investigate the scope for **PD** to **PE** conversion inside the cavity of **Mn1** more directly, we designed and synthesized a polymer–porphyrin rotaxane **Mn3** as a model compound. In this molecule, the rotaxane architecture with the catalyst enclosing the polybutadiene substrate is enforced. The first alternative mechanism, the 'loop' mechanism, is thus sterically impossible; moreover, catalysis on the 'outside' of the catalyst is topologically inhibited.

The synthesis of **Mn3** is based on our earlier work in which the strong affinity of **Mn1** for **V** is used to form a pseudo-rotaxane structure that is subsequently capped with a suitable stopper to form a rotaxane[17]. Using this approach, bis-bipyridyl-appended polybutadiene (**bipy$_2$PD**) was treated with 2 equiv. of porphyrin **Mn1** to yield pseudo-rotaxane **Mn1**:**bipy$_2$PD**:**Mn1**, which was subsequently capped with a 3,5-di-*tert*-butylphenyl derivative to obtain the target polymer-porphyrin-[3]-rotaxane **Mn3** in approximately 43% yield (Supplementary Information).

Catalytic studies using the [3]-rotaxane **Mn3** both in the presence and in absence of the **tbpy** ligand were carried out as described above and the results compared with those obtained using the porphyrin clips **Mn1** and **Mn2**. It should be noted that in the case of rotaxane **Mn3**, the substrate (polybutadiene) is now part of the molecule, whereas in the other cases the related polybutadiene **bipy$_2$PD** was used as the substrate. The substrate/catalyst ratio in the pseudo-rotaxane systems is fixed by the ratio of the two components in the **Mn3** rotaxane, which is ~40. We used substrate concentrations below 10 mM, thus suppressing intermolecular side reactions but also obtaining lower turnover numbers (Table 1,

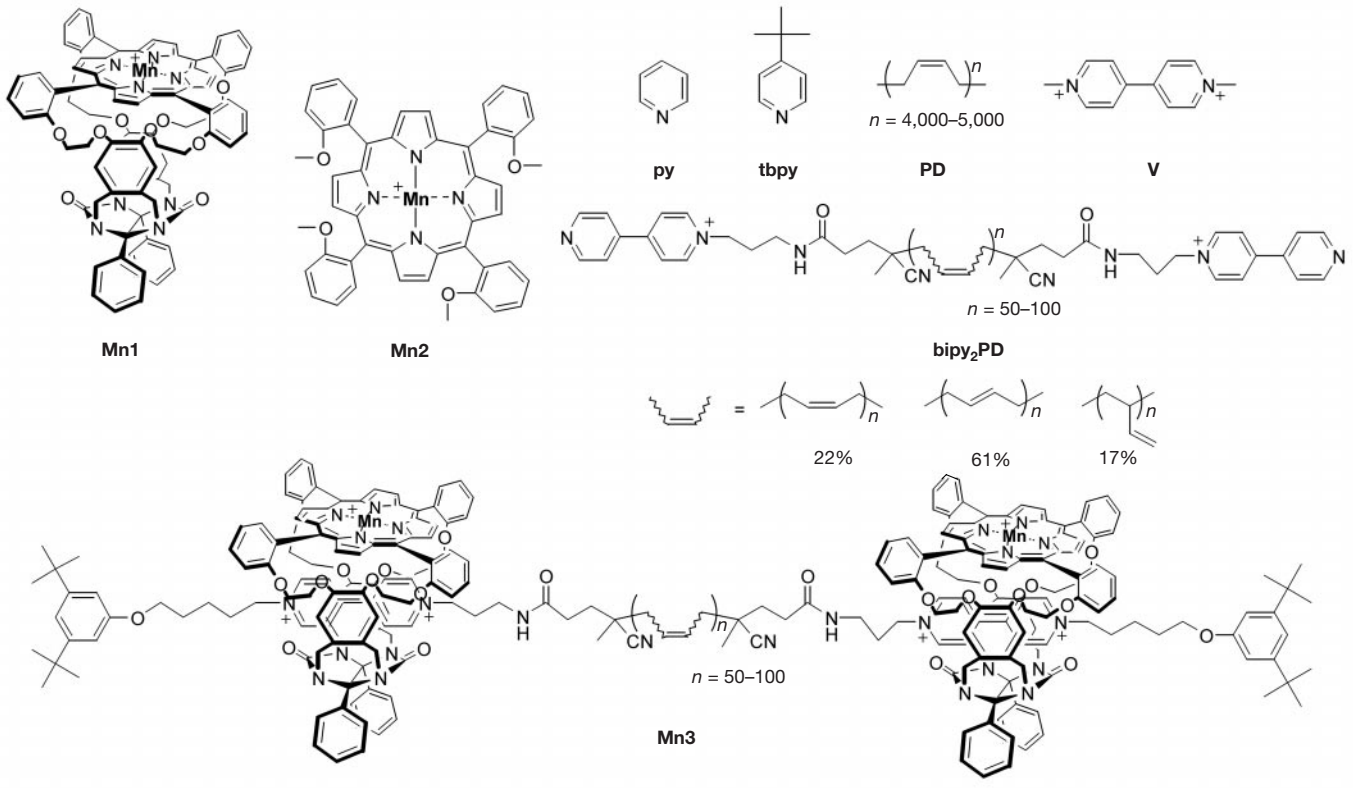


**Figure 2** Structural formulae of the catalysts, substrates and ligands used in this work.

Table 1 **Catalytic activities of manganese(III) porphyrins**

| Entry | Catalyst | Substrate | [C = C] (mM) | [C = C]/[catalyst] | Turnover number (h) tbpy | Turnover number (h) No ligand |
|---|---|---|---|---|---|---|
| 1 | **Mn1** | **PD** | 250 | 250 | 140 | – |
| 2 | **Mn1:V*** | **PD** | 250 | 250 | 85 | – |
| 3 | **Mn2** | **PD** | 250 | 250 | 310 | – |
| 4 | **Mn2:V*** | **PD** | 250 | 250 | 375 | – |
| 5 | **Mn1** | **PD** | 8 | 42 | 15 | 21 |
| 6 | **Mn1** | **bipy$_2$PD** | 8 | 43 | 7 | 20 |
| 7 | **Mn2** | **bipy$_2$PD** | 8 | 42 | 21 | 10 |
| 8 | **Mn3** | **Mn3**† | 6 | 37 | 12 | 5 |
| 9 | **Zn1**‡ | **bipy$_2$PD** | 8 | 45 | 0 | – |

[C = C] = concentration of double bonds in **PD** (Acros, $M_w \sim 300{,}000$, 98% *cis*), **bipy$_2$PD** (Aldrich, $M_w \sim 4{,}500$; 22% 1,4-*cis*-, 61% 1,4-*trans*-, and 17% 1,2-butadiene) and **Mn3** ($M_w \sim 9{,}000$, based on **bipy$_2$PD**). See Fig. 2 for structures and abbreviations and Methods for experimental details. Turnover number = ([substrate converted]/[catalyst]). For **Mn3**, [catalyst] = concentration of Mn(III) porphyrin (2 × [**Mn3**]).
*1 equiv. of **V** added.
†In **Mn3**, the catalyst and substrate are topologically linked.
‡**Zn1** is the zinc(II) analogue of **Mn1**[18] and was used as a control to prove that PhIO does not carry out oxidation reactions in the absence of manganese(III) porphyrin.

entries 5–9). The activity of our system is, however, still comparable to that measured for naturally occurring oxidative systems such as the enzyme Cytochrome P450 (0.1–60 turnovers per catalyst per hour)[24,25].

In the presence of the **tbpy** ligand, the polymeric porphyrin-rotaxane **Mn3** is a more effective catalyst (~2 × higher turnovers per hour) than the pseudo-rotaxane system **Mn1**-**bipy$_2$PD** (Table 1, entries 6 and 8). We attribute the increased activity to the enforced rotaxane topology of **Mn3** (Fig. 1f), which ensures that the initial binding of the catalyst to the substrate is already achieved. In line with the inhibition experiments discussed above, the turnover frequency for the conversion of **bipy$_2$PD** by **Mn1** is 50% lower than that of **PD** by **Mn1** (Table 1, entries 5 and 6), indicating that the bipyridine-endgroups of the **bipy$_2$PD** substrate bind strongly in the cavity and inhibit catalysis (compare to Table 1, entries 1 and 2). The catalytic turnover of **Mn1** is lower in the presence of **tbpy** than in the absence of **tbpy** (~65% lower, entry 6 in Table 1), whereas rotaxane **Mn3** exhibits about twice the catalytic activity when **tbpy** is bound (entry 8 in Table 1). This observation is explained by the fact that a pyridine axial ligand enhances the catalytic activity of Mn(III) porphyrins[19], as also seen with **Mn2** (~2 × higher, entry 7 in Table 1). With **Mn1**, when the axial ligand is present, catalytic conversion of the polymer substrate **bipy$_2$PD** takes place 'inside' the catalyst cavity, making the reaction sterically demanding; once the ligand is absent, reaction occurs more rapidly on the 'outside' of the catalyst. The polymer rotaxane **Mn3**, on the other hand, requires the **tbpy** ligand for activation and is considerably less active in the absence of **tbpy**. These results highlight that the **tbpy** ligand remains bound under the catalytic conditions used and that catalysis occurs inside the cavity of rotaxane **Mn3** (Fig. 1f).

Further support for the rotaxane mechanism was obtained from a study of the relative reactivities of the olefinic double bonds in the **bipy$_2$PD** substrate (also the thread in **Mn3**). In contrast to **PD**, this polymer is a mixture of *cis*-1,4-butadiene, *trans*-1,4-butadiene and 1,2-butadiene units (Fig. 2) that differ in their reactivities towards oxidation by the Mn(III) porphyrin catalysts, with the *cis*-isomers generally being more reactive than the *trans*-isomers[19]. The ratios of the *trans*-epoxide/*cis*-epoxide products obtained with the different catalysts was measured by $^1$H NMR after 30% total conversion of the polymeric substrate (Table 2). In the presence of **tbpy**, the highest *trans*/*cis* ratio was found for the rotaxane **Mn3** and the lowest for **Mn2** with **Mn1** displaying an intermediate ratio. All three catalysts showed a more similar product ratio in the absence of **tbpy** (*trans*/*cis* ratio = 1.0 ± 0.4). These results are again in line with the idea that in the case of **Mn1** and **Mn3**, catalysis occurs preferentially or completely within the cavity of the catalysts. To estimate the extent to which catalysis occurs inside and outside **Mn1**, we carried out control epoxidation reactions using a **Mn1** derivative, in which the cavity is completely blocked in a rotaxane architecture (**Mn4**, see Supplementary Information S-7). These experiments revealed that for the catalytic system **Mn1**-**PD**, 80% of the polymer conversion occurs inside **Mn1** and for the polymer system **Mn1**-**bipy$_2$PD** 45% inside. This latter value is in good agreement with the 55% conversion inside **Mn1**, obtained from the analysis of the product *cis*/*trans* ratios (see Supplementary Information S-7). This lower percentage conversion inside the cavity of **Mn1**, for the **Mn1**-**bipy$_2$PD** system is probably the result of the endgroups of the polymeric substrate binding and partially inhibiting catalysis inside the toroid.

Table 2 **Chemo- and stereo-selectivities of reactions**

| Substrate | Catalyst | Polyepoxides formed *cis* | Polyepoxides formed *trans* | *trans*/*cis* ratio |
|---|---|---|---|---|
| **PD*** | **Mn1** | 20% | 80% | 4.0 |
| **PD*** | **Mn2** | 78% | 22% | 0.3 |
| **bipy$_2$PD**† | **Mn1** | 37% | 63% | 1.7 |
| **bipy$_2$PD**† | **Mn2** | 59% | 41% | 0.7 |
| **Mn3**† | **Mn3** | 20% | 80% | 4.0 |

All reactions were carried out at [C = C] of 6–8 mM in the presence of 500-fold excess of **tbpy**. See Table 1 for abbreviations and Methods for experimental details.
*This substrate (**PD**) contains >98% *cis*-butadiene bonds.
†These substrates (**bipy$_2$PD** and **Mn3**) contain 22% 1,4-*cis*-, 61% 1,4-*trans*- and 17% 1,2-butadiene double bonds (Fig. 2), giving a *trans*/*cis* ratio of 2.8 in the starting product.

It is unclear at this stage whether the catalytic process is sequentially processive or random, that is, whether the catalyst moves step by step along the chain or hops randomly. Calculated from the rate of the reaction and taking into account the length of the polymer, the catalyst would move around 1–700 pm s$^{-1}$ (the lower value if the reaction is sequential, the higher one if it is random) which is not very dissimilar to the speed of RNA polymerase (3,000 pm s$^{-1}$)[26] but is low when compared to the speeds that can be calculated from data published on synthetic rotaxane shuttles (several μm s$^{-1}$)[27].

Experiments were also carried out with NaOCl as oxidant in a two-phase system of dichloromethane and water ($CH_2Cl_2/H_2O$). Using the conditions of entries 1–4 in Table 1, greatly enhanced activities were found for the cavity containing catalyst **Mn1** with turnover frequencies >500 h$^{-1}$ for the conversion of **PD** to **PE**. This improved performance is thought to be a combination of the different nature of the oxidant used, and possibly the fact that the hydrophilic **PE** chain is pulled into the water phase as it forms during reaction, creating an additional driving force for the reaction (see Supplementary Fig. S2). Unfortunately, no decisive conclusions could be made about the mechanism in this two-phase system, because experiments with rotaxane **Mn3** were unsuccessful—the stoppers were cleaved off under the strongly basic reaction conditions (pH ~13)[28], destroying the rotaxane topology.

The results presented here show that catalytic modifications of a polymer can be realized using a catalyst that is topologically linked to its substrate. To make the system sequentially processive, one has to precisely balance the speed of the movement of the catalyst and the catalytic rate of the reaction, which in the present case is probably too slow when compared to the former process. Nevertheless, the rotaxanes **Mn1**:**PD** and **Mn3** are initial attempts to mimic the naturally occurring toroidal enzyme systems such as the various exo- and endonucleases. Processive rotaxane catalysis may open a new route, at least in principle, to carry out post-polymerization transformations on various functional polymers, either synthetic or biological. □

## Methods

Catalytic activities were determined as follows: in a typical experiment the oxidant (1–2 equiv. PhIO) was added to a deuterated chloroform solution (1.0 ml) containing the porphyrin and polymer and when appropriate, the **tbpy** (500 × [porphyrin]) ligand

under an argon atmosphere. For experiments with **Mn3**, a concentration of [**Mn3**] = 0.08 mM was used (on the basis of the relative molecular mass, $M_w$, of **Mn3** this gives [porphyrin] = 0.16 mM and [C = C] = 6 mM) and when appropriate the ligand **tbpy** in a concentration of [**tbpy**] = 81 mM. The resulting mixture was magnetically stirred at 1,100 r.p.m. Samples were taken which were filtered (to remove excess of iodosylbenzene) and the resulting filtrates were analysed by $^1$H-NMR. In the case of **Mn3** and **bipy$_2$PD** only the protons of the *cis*- and *trans*-1,4-polybutadiene (5.8–5.2 p.p.m.) and *cis*- and *trans*-1,4-polyepoxide (3.0–2.6 p.p.m.) were used to calculate the conversion of the substrate. Turnover frequencies were calculated from data points up to ~30% conversion, since in a number of cases at higher conversions, deviations from first-order behaviour in substrate (alkene) concentration were observed. See Supplementary Information for further experimental details.

Received 19 February; accepted 17 July 2003; doi:10.1038/nature01925.


1. Breyer, W. A. & Matthew, B. M. A structural basis for processivity. *Protein Sci.* **10,** 1699–1711 (2001).
2. Kool, E. T., Morales, J. C. & Guckian, K. M. Mimicking the structure and function of DNA: Insights into DNA stability and replication. *Angew. Chem. Int. Edn Engl.* **39,** 990–1009 (2000).
3. Benkovic, S. J., Valentine, A. M. & Salinas, F. Replisome-mediated DNA replication. *Annu. Rev. Biochem.* **70,** 181–208 (2001).
4. Lin, S. M., Lloyd, R. S. & Roberts, R. J. *Nucleases*, 2nd edn (Cold Spring Harbor Laboratory Press, Cold Spring Harbor, NY, 1993).
5. Kool, E. T. Recognition of DNA, RNA, and proteins by circular oligonucleotides. *Acc. Chem. Res.* **31,** 502–510 (1998).
6. Trakselis, M. A., Alley, S. C., Abel-Santos, E. & Benkovic, S. J. Creating a dynamic picture of the sliding clamp during T4 DNA polymerase holoenzyme assembly by using fluorescence resonance energy transfer. *Proc. Natl Acad. Sci. USA* **98,** 8368–8375 (2001).
7. Kovall, R. & Matthews, B. W. Toroidal structure of lambda-exonuclease. *Science* **277,** 1824–1827 (1997).
8. Ashton, P. R. *et al.* A light-fueled "piston cyclinder" molecular-level machine. *J. Am. Chem. Soc.* **120,** 11190–11191 (1998).
9. Sauvage, J.-P. Transition metal-containing rotaxanes and catenanes in motion: towards molecular machines and motors. *Acc. Chem. Res.* **31,** 611–619 (1998).
10. Davis, A. P. Synthetic molecular motors. *Nature* **401,** 120–121 (1999).
11. Schalley, C. A., Beizai, K. & Vögtle, F. On the way to rotaxane-based molecular motors: studies in molecular mobility and topological chirality. *Acc. Chem. Res.* **34,** 465–476 (2001).
12. Bissell, R. A., Córdova, E., Kaifer, A. E. & Stoddart, J. F. A chemically and electrochemically switchable molecular shuttle. *Nature* **369,** 133–137 (1994).
13. Jiménez, M. C., Dietrich-Buchecker, C. & Sauvage, J.-P. Towards synthetic molecular muscles: Contraction and stretching of a linear rotaxane dimer. *Angew. Chem. Int. Edn Engl.* **39,** 3284–3287 (2000).
14. Collier, C. P. *et al.* Electronically configurable molecular-based logic gates. *Science* **285,** 391–394 (1999).
15. Harada, A., Li, J. & Kamachi, M. The molecular necklace: a rotaxane containing many threaded α-cyclodextrins. *Nature* **356,** 325–327 (1992).
16. Shen, Y. X., Xie, D. & Gibson, H. W. Polyrotaxanes based on polyurethane backbones and crown ether cyclics. 1. Synthesis. *J. Am. Chem. Soc.* **116,** 537–548 (1994).
17. Rowan, A. E., Aarts, P. P. M. & Koutstaal, K. W. M. Novel porphyrin-viologen rotaxanes. *Chem. Commun.*, 611–612 (1998).
18. Elemans, J. A. A. W. *et al.* Porphyrin clips derived from diphenylglycoluril. Synthesis, conformational analysis, and binding properties. *J. Org. Chem.* **64,** 7009–7016 (1999).
19. Meunier, B. Metalloporphyrins as versatile catalysts for oxidation reactions and oxidative DNA cleavage. *Chem. Rev.* **92,** 1411–1456 (1992).
20. Elemans, J. A. A. W., Bijsterveld, E. J. A., Rowan, A. E. & Nolte, R. J. M. A host-guest epoxidation catalyst with enhanced activity and stability. *Chem. Commun.*, 2443–2444 (2000).
21. Tornaritis, M. J. & Coutsolelos, A. G. Metalloporphyrins catalyse cis-polybutadiene to polyepoxide. *Polymer* **33,** 1771–1772 (1992).
22. Sacco, H. C., Iamamoto, Y. & Lindsay Smith, J. R. Alkene epoxidation with iodosylbenzene catalysed by polyionic supports. *J. Chem. Soc. Perkin Trans.* **2,** 181–190 (2001).
23. Tsuda, Y., Takahashi, K., Yamaguchi, T., Matsui, S. & Komura, T. Catalytic epoxidation of cyclohexene by covalently linked manganese porphyrin-viologen complex. *J. Mol. Catal. A: Chem.* **130,** 285–295 (1998).
24. Hollis, B. W. 25-Hydroxyvitamin $D_3$-1α-hydroxylase in porcine hepatic tissue: Subcellular localization to both mitochondria and microsomes. *Proc. Natl Acad. Sci. USA* **87,** 6009–6013 (1990).
25. Guengerich, F. P. Reactions and significance of cytochrome P-450 enzymes. *J. Biol. Chem.* **266,** 10019–10022 (1991).
26. Perkins, T. T., Mitsis, P. G., Dalal, R. V. & Block, S. M. Watching enzymes move along DNA one at a time. *Biophys. J.* **80,** 1464 Part 2 (2001).
27. Brouwer, A. M. *et al.* Photoinduction of fast, reversible translational motion in a hydrogen-bonded molecular shuttle. *Science* **291,** 2124–2128 (2001).
28. Farrington, J. A., Ledwith, A. & Stam, M. F. Cation-radicals: Oxidation of methoxide ion with 1,1′-dimethyl-4,4′-bipyridylium dichloride (paraquat dichloride). *J. Chem. Soc. Chem. Commun.*, 259–260 (1969).


**Supplementary Information** accompanies the paper on **www.nature.com/nature**.

**Acknowledgements** We thank J. Foekema and I. M. Dixon for preliminary studies and discussions. This research was supported by a NRSC Catalysis grant, a NWO Vidi grant (A.E.R.) and an EC Marie Curie fellowship (P.T.).

**Competing interests statement** The authors declare that they have no competing financial interests.

**Correspondence** and requests for materials should be addressed to A.E.R. (rowan@sci.kun.nl).

# Extreme deuterium enrichment in stratospheric hydrogen and the global atmospheric budget of $H_2$

**Thom Rahn[1]*, John M. Eiler[1], Kristie A. Boering[3,4], Paul O. Wennberg[1,2], Michael C. McCarthy[3], Stanley Tyler[5], Sue Schauffler[6], Stephen Donnelly[6] & Elliot Atlas[6]**

[1]*Division of Geological and Planetary Sciences, and* [2]*Division of Engineering and Applied Sciences, California Institute of Technology, Pasadena, California 91125, USA*
[3]*Department of Chemistry, and* [4]*Department of Earth and Planetary Science, University of California at Berkeley, Berkeley, California 94720, USA*
[5]*Earth Systems Science Department, University of California, Irvine, Irvine, California 92697, USA*
[6]*National Center for Atmospheric Research, Boulder, Colorado 80307-3000, USA*

* Present address: Los Alamos National Laboratory, EES-6, MS-D462, Los Alamos, New Mexico 87545, USA

**Molecular hydrogen ($H_2$) is the second most abundant trace gas in the atmosphere after methane[1] ($CH_4$). In the troposphere, the D/H ratio of $H_2$ is enriched by 120‰ relative to the world's oceans[2–4]. This cannot be explained by the sources of $H_2$ for which the D/H ratio has been measured to date (for example, fossil fuels and biomass burning)[5,6]. But the isotopic composition of $H_2$ from its single largest source—the photochemical oxidation of methane—has yet to be determined. Here we show that the D/H ratio of stratospheric $H_2$ develops enrichments greater than 440‰, the most extreme D/H enrichment observed in a terrestrial material. We estimate the D/H ratio of $H_2$ produced from $CH_4$ in the stratosphere, where production is isolated from the influences of non-photochemical sources and sinks, showing that the chain of reactions producing $H_2$ from $CH_4$ concentrates D in the product $H_2$. This enrichment, which we estimate is similar on a global average in the troposphere, contributes substantially to the D/H ratio of tropospheric $H_2$.**

$H_2$ has been proposed as the basis for fuel-cell technologies that are anticipated to expand substantially in coming decades, and, as with fossil fuels, there is potential for significant leakage from the requisite infrastructure[7,8]. The consequences of a new source of $H_2$ to the atmosphere are not easily anticipated, and preparation for potential change must begin with a precise and accurate description of the global budget. Stable isotope measurements are often used to constrain the budgets of atmospheric trace gases, but have seen limited use for $H_2$ owing to analytical difficulties and lack of data on its isotopically distinct sources and sinks. Major sources having known isotopic compositions (fossil-fuel combustion, biomass burning, $H_2$-producing metabolisms) have $\delta D_{H2}$ values ranging from −800‰ to −250‰ (refs 2–6), far lower than the average tropospheric value of about +120‰ (refs 2–4, 9). It has been argued that this difference could be caused by the slower rate of photochemical oxidation of HD compared to HH (if $H_2$ oxidation is the major tropospheric sink)[10], or by enrichment of D in $H_2$ produced via oxidation of methane ($CH_4$) and/or non-methane hydrocarbons (if uptake by soils is the major tropospheric sink)[5]. Records of $H_2$ concentration[1,11] show greater seasonal amplitude and lower average concentration in the Northern Hemisphere, implying an atmospheric lifetime of ~2 yr and requiring uptake by soils to be the major sink[1]. Thus, either photochemical production is indeed responsible for the observed D enrichment or our understanding of the $H_2$ budget is incomplete.

Oxidation of atmospheric $CH_4$ consists of a chain of reactions that include $H_2$ as one of the products (Fig. 1). Although roughly 90% of this photochemical $CH_4$ loss occurs in the troposphere, we